



Iron-copper mineralization associated with metagabbro in Mirawa Village, Kurdistan region, northeastern Iraq

Irfan Omar Mousa Yara¹ & Yousif Osman Mohammad¹

1Department of Geology, College of Science, University of Sulaimani, Iraq

Qlyasan Campus, Sulaimani-Kirkuk Main Road

irfan.mosa@univsul.edu.iq

Article info

Original: 22 February 2018
 Revised: 12 May 2018
 Accepted: 11 June 2018
 Published online: 20 June 2018

Key Words:

*Iron-copper
 Mineralization
 Metagabbro
 Geothermometry*

Abstract

Mirawa iron-copper mineralization in Mirawa village, Kurdistan region, occurs as a zone of 15 m thick within the metagabbro of the Mawat Ophiolite. It is hosted by brecciated amphibolite facies gabbroic rocks with a northwest–southeast trending shear zone. Amphibole, magnetite, plagioclase, quartz, epidote, chlorite, clinopyroxene and chalcopyrite represent the mineral constituents of metagabbro. Metamorphic conditions have been estimated from the green metamorphic amphibole replacing primary magmatic clinopyroxene (M1, 500 < T < 560 °C; 4.3 < P < 5.2 kbar) and retrograde actinolite (white amphibole) replacing the green amphibole due to continuous decreasing pressure and temperature (M2, 415 < T < 480 °C; 1.9 < P < 2.3 kbar). Occurrence of quartz with iron-copper mineralization hydrothermal fluids played a significant role during metamorphism. Chlorite and epidote were formed at the late stage of metamorphism.

Iron-copper mineralization occurred in two paragenetic stages. Coarse grains of magnetite, chalcopyrite and pyrite formed during the first stage of mineralization representing syngenetic mineralization. Magnetite is the main Fe-ore mineral and it is characterized by large euhedral to subhedral grains with ilmenite exsolution lamellae. The second stage is epigenetic where mineralization is characterized by the formation of secondary minerals, replacing the primary minerals. Hematite replaces primary magnetite along the rim. Chalcopyrite, pyrite and magnetite were replaced by goethite whereas covellite overgrows chalcopyrite forming a corona texture. Fine-grained idiomorphic aggregates of magnetite are dominant in the second stage and seem to be formed from iron liberated from pyroxene and other iron-bearing minerals. Microstructural orientation of the coarse-grained magnetite indicates a NW-SE direction for the maximum stretching of strain ellipse.

Introduction

The Zagros orogen is subdivided into three parallel belts, these are; from northeast to southwest (Fig. 1), the Tertiary Urumieh-Dokhtar magmatic belt [1] and [2], the Sanandaj-Sirjan tectonic zone [3], [4] and [5], the Zagros Fold Belt (ZFB) [6], [3] and [4]. The ZFB in Iraqi-Kurdistan can further be divided, from the northeast to the southwest, into three parallel NW-SE-trending structural domains, these are i) the Zagros Suture Zone (ZSZ), ii) the High Folded Zone, and iii) the Foot Hill Zone (Fig. 1; [7] and [8]). Copper occurrences are wide spread all over the area of the Zagros Suture Zones, but only a few of them may be of economic interest. The distribution of mineral deposits of Kurdistan is shown in Figure 2. Many of these occurrences are related to the serpentized ultramafic rocks and gabbros of Penjween, Mawat and Bulfat massives. Mawat area is characterized by a variety of metallic mineral deposits of Cu, Cr, and Mn (Fig. 2). [9] Outlined a zone of low value copper deposits near Waraz Police Post after which was named copper hill.

The country rock consists of diorite with intrusions of quartz and brown schistose epidiosite. [9] Considered the origin of the copper by hydrothermal processes and also showed that the copper content varies from (0.01% to 0.04%). [10] and [11] reported many copper mineralizations from the crush zone in gabbro SW of Korradawi Village and from granodiorites, pyroxenites and gabbros south of Konjrin Village. The mineralization consists of chalcopyrite, pyrite, malachite and azurite, with Cu content between (2.84 and 23%). The main aim of this work is to study the origin of copper-iron mineralization, petrogenesis and metamorphic evolution in Mirawa area in the Mawat igneous complex using petrographic and geochemical methods.

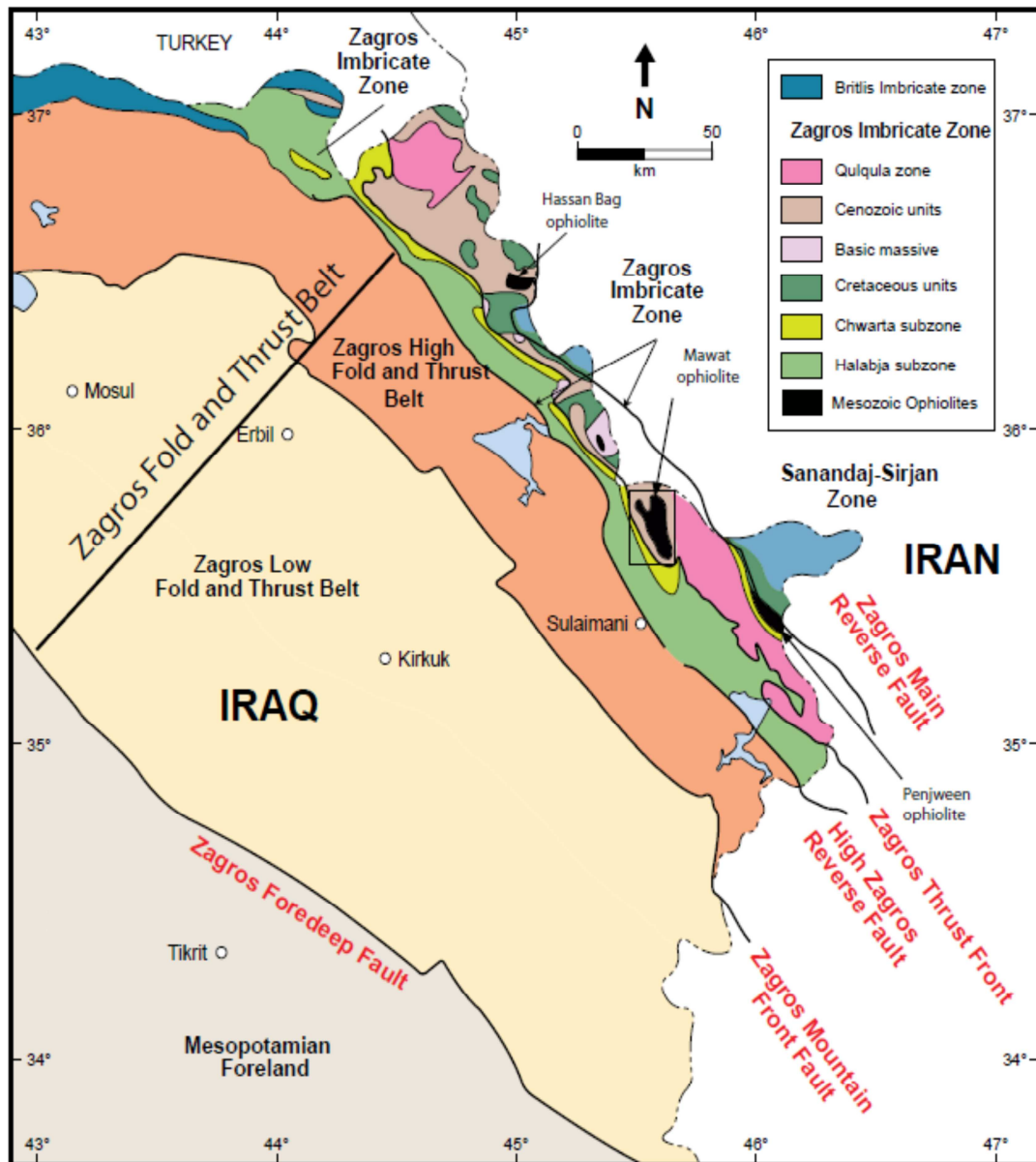


Figure 1: Regional tectonic map of northeastern Iraq showing the distribution of Mesozoic Neo-Tethyan ophiolites (after [12]).

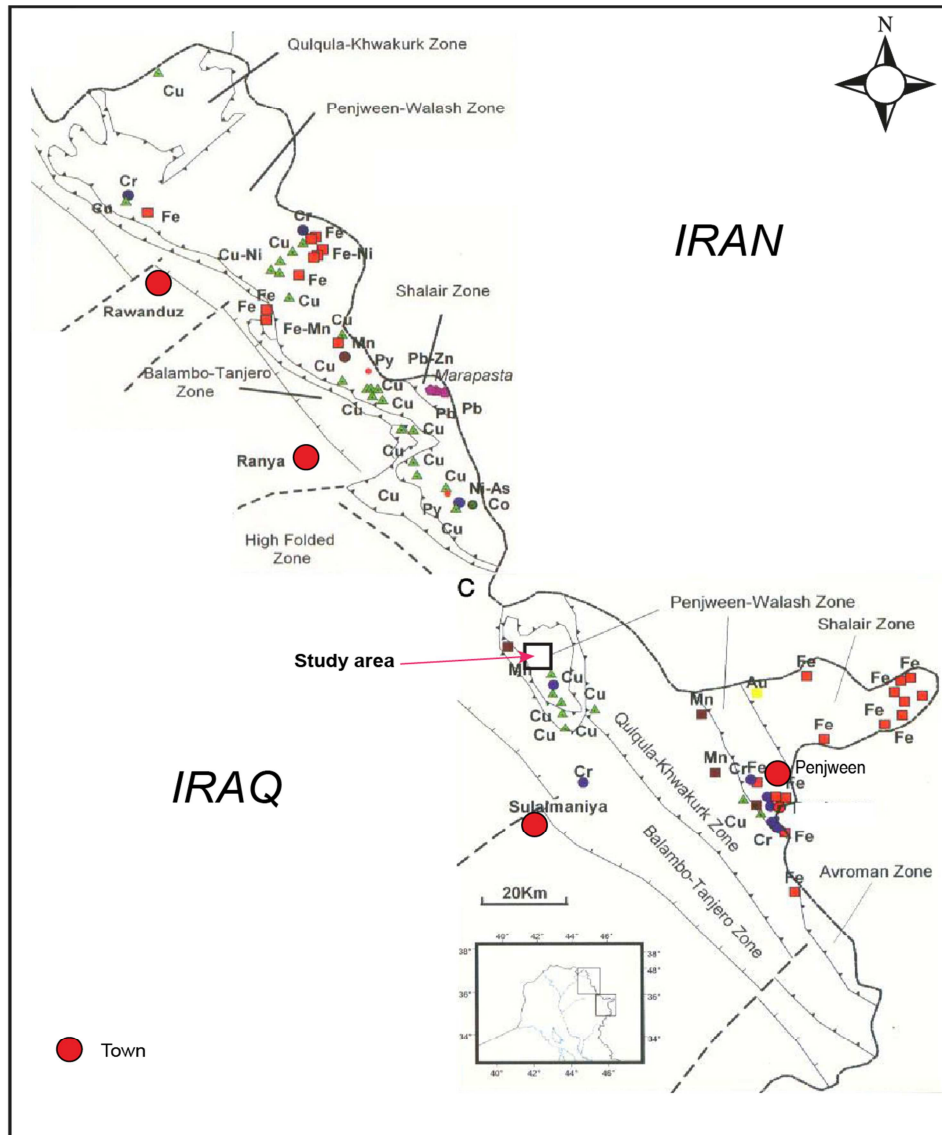


Figure 2: Location of the study area and distribution of the metallic mineralizations in the eastern parts of Kurdistan (after [13]).

Regional Geology

Mirawa is located within the Mawat ophiolite complex, specifically in the western part of Mawat ophiolite. The ophiolite of Mawat covers about 250 km² within the Iraqi Zagros sutures zone (IZSZ) [7] northeast Iraq 35 km northeast Sulaimani city , and it represents one of the complexes of the Neo-Tethyan ophiolite and part of croissant ophiolite [14] that extends from Semail ophiolite of Oman to Troodos ophiolite of Cyprus passing through Iraq , Iran , Turkey and Syria (Fig.1) .

The ophiolite comprises the upper thrust sheet of Mawat nappe (Albian – Cenomanian) [15] and [7] consists of 600 – 1000 m of basaltic , and meta basalt intruded by plutonic complexes of ultrabasic pyroxenite , layered and massive gabbros , diorite , dolerite dikes and late stage plagiogramite (fig. 3). The gabbro is the largest unit including banded gabbro intruded to the east by coarse massive gabbros. This is followed by ultramafics dunite and peridotite which are variably serpentized. The western contacts of the banded gabbro with the metavolcanics a form north – south trending shear zone and along this shear zone the gabbro is highly deformed, brecciated and intruded by basic and acidic intrusions [16] , [17] and [18]. The gabbro

was thrust onto the metavolcanics during the final stages of solidification resulting in marginal shearing along the contact.

There is a general agreement that the Mawat ophiolite represents a Mesozoic subduction type of ophiolite formed in a forearc shortly after initiation of subduction and it is geochemically correlated with the Oman and Troodos ophiolites [19],[20] , [21] , and [12]. Meanwhile, [22] suggested a mantle plume origin for the Mawat ophiolite. This controversy is mainly due to the absence of an up to-date solid geological map of the area, as the area till now is politically unstable region and the only available geological mapping in the area is from the mid twentieth century. Moreover the main mafic-ultramafic rock units were not mapped accurately. The ultramafic unit shows typical characteristics of alpine-type peridotite [20]. Small bodies of medium- to coarse-grained leucogranite consisting of quartz, plagioclase, alkali feldspar, and tourmaline are found in the ultramafic unit. The volcanic unit is found is one small outcrop in the southern part of the Mawat ophiolite near Waraz village.

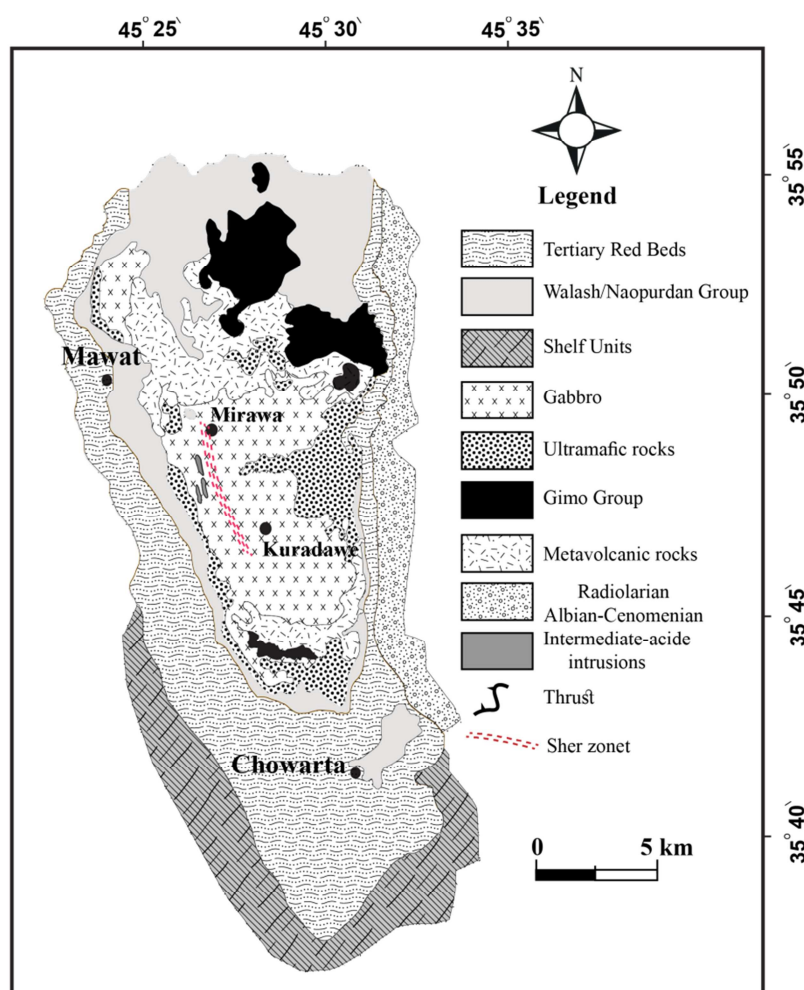


Figure 3: Geological map of the Mawat ophiolite complex, northeastern Iraq, modified from [23].

Sampling and analysis techniques

Eighteen samples of mineralization and associated metagabbro samples were collected from the area in two field trips. Twenty three thin sections are made along the various directions of the samples and investigated by transmitted light polarizing microscope for textures and mineral identifications. Ten mount polished sections were prepared for the mineralization. All polished sections were studied by reflected light polarizing microscope for texture and mineral identifications. Two mount polished sections were selected for chemical composition of the constituent minerals by Scanning Electron Microscopy (SEM) at TU Bergakademie

Freiberg. Acceleration voltage was 15 kV and the beam current was at 20 nA with the beam focussed in a 2 μm diameter spot. Geothermobarometry and P-T conditions were calculated for the metagabbro using the chemical composition of the amphibole equilibrium according to [24].

Field occurrence and petrography

Near the southern part of Merawa village along the main road, seven meters of dark reddish green schist occur within the gabbro unit of Mawat ophiolite complex. This rock is characterized by fine to medium grain size. On the outcrop it is foliated dark reddish green in color. Eighteen samples were collected for petrographic and mineralogical examination to determine the origin of the mineralization. Under the microscope the studied samples consists mainly of amphibole (hornblend, tremolite-actinolite), chlorite, magnetite, epidote, plagioclase and quartz. Two types of amphibole are distinguished, fibrous (tremolite-actinolite) and prismatic with anhedral to subhedral crystals. Amphiboles show transformed from preexisting pyroxene due to metamorphism. The fibrous amphibole is more abundant and it's formed due to intense deformation of preexisting pyroxene and amphibole along their edges (Fig. 4a) [25]. Poikiloblastic textures are observed from less fibrous amphibole enclosing opaque mineral grains (Fig. 4b). Late fibrous amphibole shows overprinting of on early plagioclase. Thus, fibrous amphibole appears to have formed during a second metamorphic episode accompanied by deformation. (Fig. 4c). Due to metamorphism, deformation and saussuritization processes most of the plagioclase crystals are altered and replaced by fine grained massive epidote (Fig. 3d). Some plagioclase grains show recrystallization to fine grains and occur along micro-shear zone and fractures as well as at grain mantles (Fig. 4e). Secondary lenticular quartz is dominant and it is characterized by andulose extinction, deformations bands and deformation lamella (Fig. 4f). Chlorite is a common mineral and formed by uralitization from amphibole or plagioclase and shows schistosity texture (Fig. 5a). The iron-copper mineralization is fine to coarse and disseminated, thus scattered irregularly inside the rocks. Sulfides and oxides are the only ore minerals found in the studied rocks. They mostly exist in the form of disseminated and small aggregates. The primary mineralogy is rather simple; sulfides are dominated by chalcopyrite as the major sulfide phase in addition to minor amounts of pyrite. Pyrite is isotropic but when the grains are subjected to high stress, they show weak anomaly of anisotropy [26], [27] and [28].

Chalcopyrite (CuFeS_2) is the only copper bearing primary mineral and shows irregular shapes scattered in the rocks or as inclusions in magnetite (Fe_3O_4) (Figs. 5b and c). Goethite ($\text{FeO}(\text{OH})$) is also observed as an alteration product of chalcopyrite, some of the chalcopyrite grains is replaced by covellite (CuS) showing rim-replacement texture (Figs. 5d and e). Magnetite represents the most abundant Fe-ore minerals. The primary oxide minerals are magnetite and ilmenite (FeTiO_3) present like as prismatic crystals, and they are observed forming exsolution texture (Fig. 5f), while goethite and hematite are secondary minerals of the primary oxides.

Small grains of chalcopyrite are enclosed within magnetite forming poikiloblastic texture (Fig. 5c). Chalcopyrite is altered to goethite and covellite forming island texture and vein-replacement textures as shown in figures (5d and 5.e) respectively. The euhedral large cubic grains of magnetite are mostly scattered throughout the groundmass and are primary oxide minerals. This reveals that the metagabbro bearing iron-copper underwent different geological environments including early magmatic and late metamorphic condition.

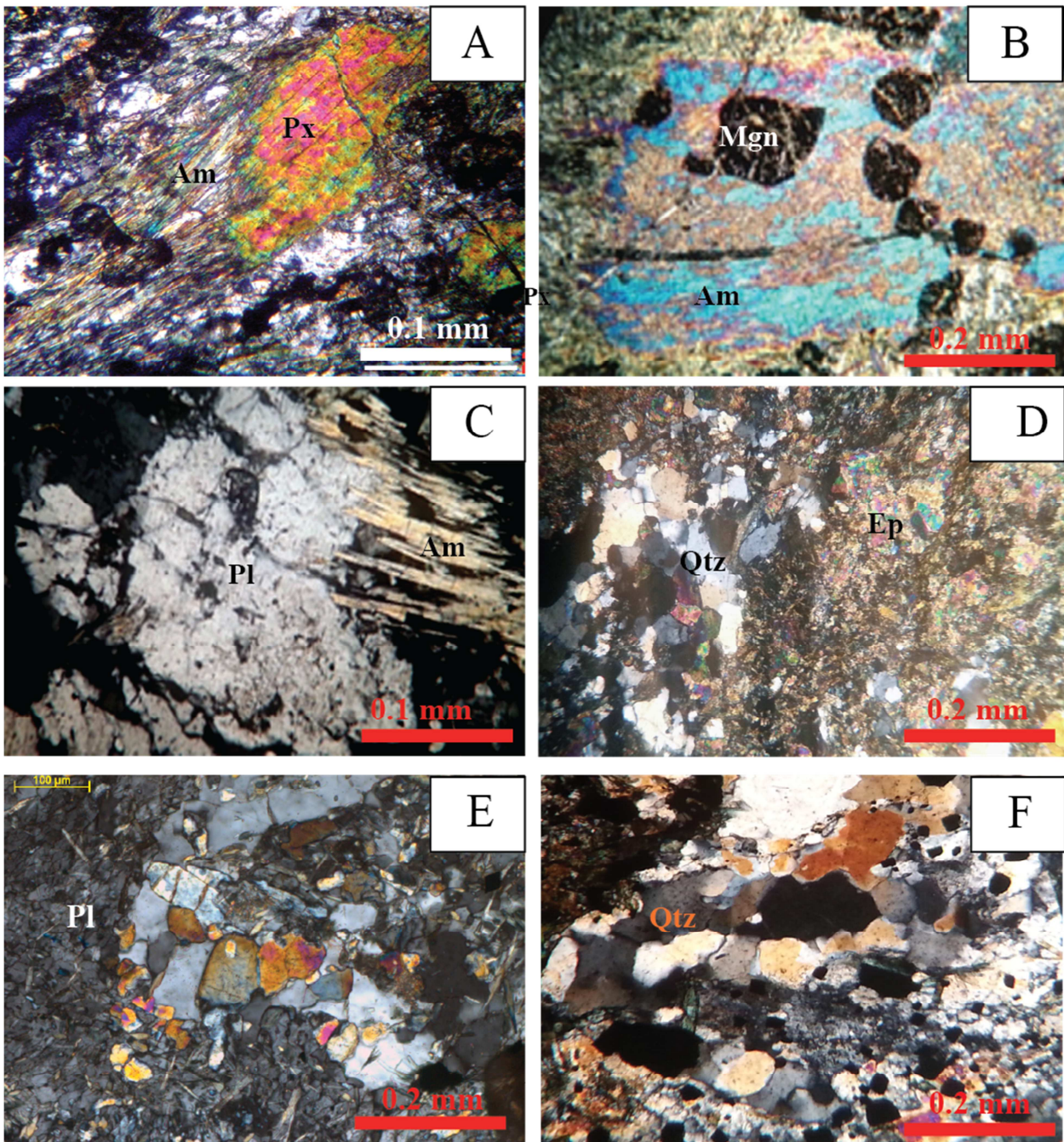


Figure 4: A) Microphotograph showing pyroxene altered to amphibole along their edge, B) Microphotograph showing Poikiloblastic textures of less fibrous amphibole enclosed opaque mineral, C) Microphotograph showing fibrous amphibole penetrating into adjacent plagioclase crystals, D) Microphotograph of plagioclase altered to massive epidote, E) Microphotograph of plagioclase show recrystallization to fine grained, F) Microphotograph of lenticular quartz showing andalous extinction. Mgn, Magnetite; Am, Amphibole; Pl, Plagioclase; Qtz, Quartz; Ep, Epidote.

Chalcopyrite shows irregular form scattered in the rocks or as inclusions in magnetite (Figs. 5b and c). Goethite is also observed as an alteration product of chalcopyrite, mean while some chalcopyrite grains are replaced by covellite along the rim (Figs. 5 d and 5e) . Magnetite represents the most abundant of the ore minerals. The primary oxide minerals are magnetite and ilmenite present as prismatic, and they are observed forming exsolution texture (Fig. 5f), while goethite and hematite are secondary minerals of the primary oxides.

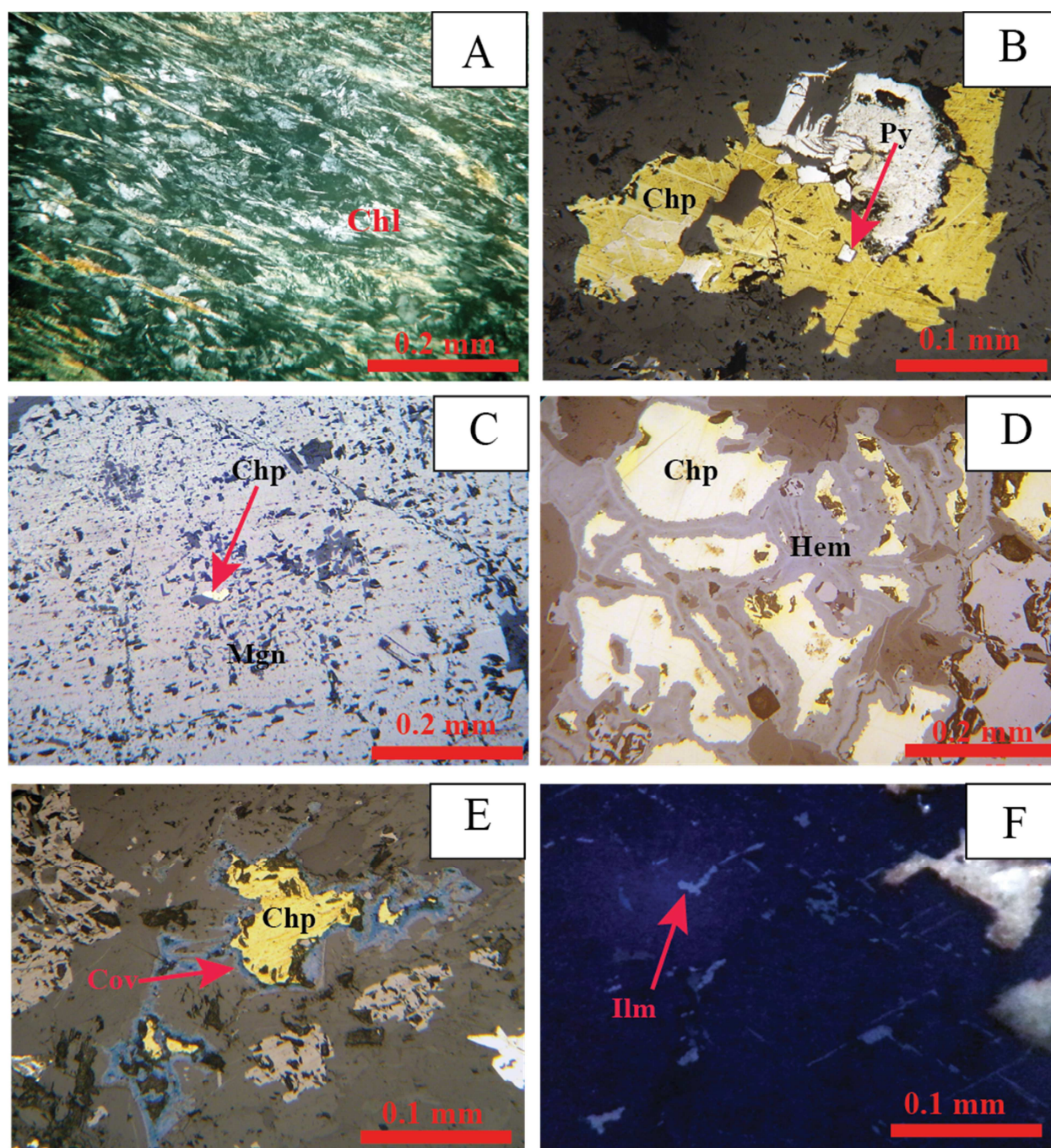


Figure 5: A) Microphotograph of chlorite showing schistosity texture, B) Microphotograph showing Chalcopyrite enclosing pyrite, C) Microphotograph showing coarse grain of magnetite enclosing chalcopyrite, D) Microphotograph showing chalcopyrite forming islands arc replacement, E) Microphotograph of covellite forming rim-replacement texture, F) Microphotograph showing exsolution between magnetite and ilmenite. Chl, Chlorite; Chp, chalcopyrite; Mgn, magnetite; Ilm, Ilmenite; Cov, covellite; Hem, Hematite; Py, Pyrite.

Mineral Chemistry

Amphibole

[29] and [30] concluded that the amphibole has various ranges of composition due to the high number of cation substitutions. Petrographic study and chemical data show the zonation in Ca-amphiboles and the grains show increase in the Si content towards the rims (Fig. 6). Optical zonation characterized by a dark

green colour in the core and pale green to color less in the rim with pleochroism in the core. Actinolite formed from hornblende and appears as a reaction rim around hornblende.

Plagioclas

Chemical data show that plagioclase is labradorite to bytownite (An₇₉₋₈₃) (Table 1). The following textures are observed in plagioclase: (a) coarse grained with undulate extinction (b) fine grained recrystallized along the fracture and around grain boundaries of the coarse grained plagioclase. Epidote is replacing plagioclase as patches are typical.

Table 1: Microprobe analyses of plagioclase from metagabbro.

Sample No.	Oxides Wt. %			
	SiO ₂	Al ₂ O ₃	CaO	Na ₂ O
b 2 pl.1	43.72	40.29	17.08	1.37
b 2 pl.2	45.76	36.58	16	1.65
b 2 pl.3	43.45	38.35	16.02	2.13
b 2 pl.4	44.07	34.99	16.71	2.34
b 2 pl.5	44	34.5	16.78	2.5
b 2 pl.6	44.03	34.78	16.68	2.59
b 2 pl.7	45.2	36.5	15.8	1.7
b 2 pl.8	45.1	36.1	15.9	1.72
b 2 pl.9	43.2	38.15	16.4	2.01
b 2 pl.10	43.6	38.01	16.1	1.99

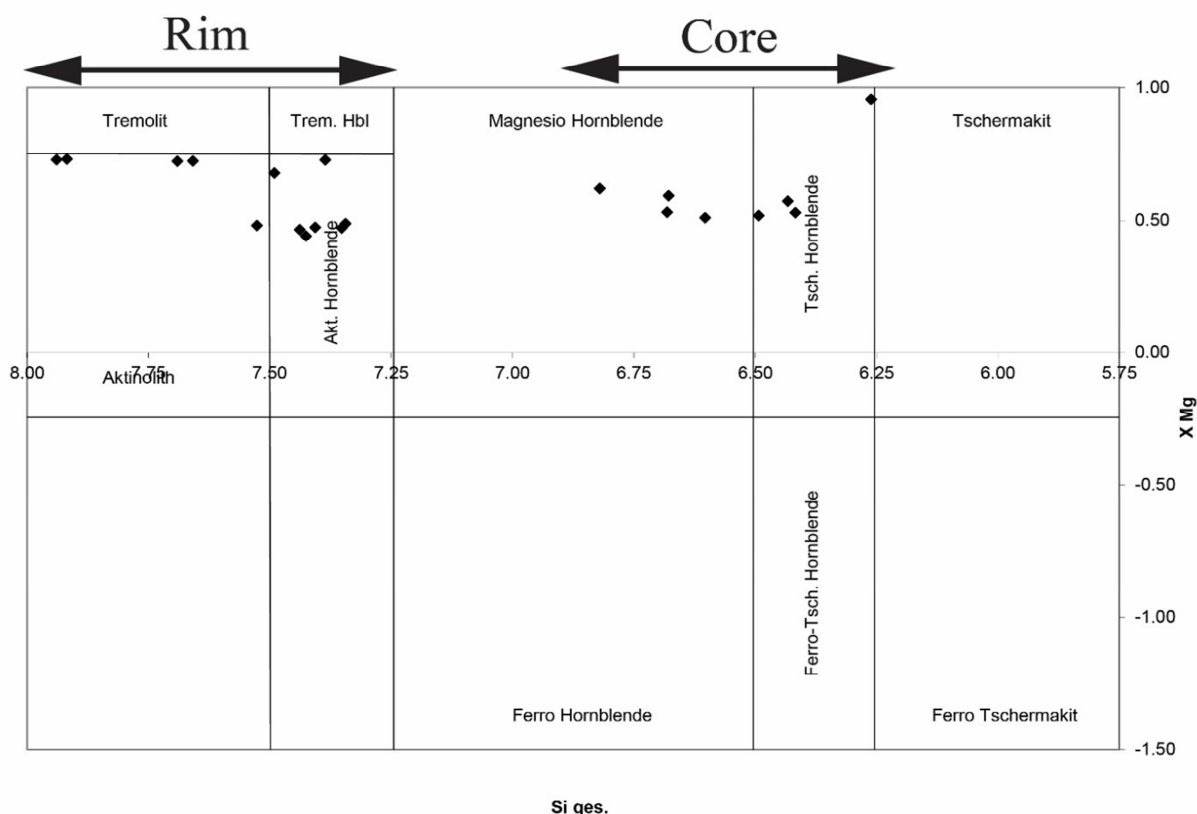


Figure 6: Si-Xmg digram showing the Composition of amphibole from metagabbroic rocks plotted on Amphibole classification digram after [29]. Xmg = Mg/(Mg+Fe).

Metamorphic evolutions

Amphibole equilibrium has been shown that metabasite mineral assemblages with growth-zoned Ca-amphiboles manifest a high potential for P–T reconstructions e.g., [31], [32] and [33]. In this work, tentative estimates are made for the P–T conditions of metagabbro in the Mirawa. Representative P–T evolutions, deduced from the chemical composition of zoned amphiboles (Table 2), are presented in Fig.7. The P–T paths reflect mainly the retrograde evolution.

Since amphibole and plagioclase are stable over a broad P–T range, thermobarometric calculations are often made using amphibole-bearing metabasic rocks [34]. Several geothermobarometers are available, based on Ca-amphibole and Ca-plagioclase [35], [36] and [37].

The polymetamorphic evolution of this metagabbroic rock through various stages has caused different mineral assemblages to form. That clearly emerges from their textures as observed in our analysis. These assemblages have been preserved in the rocks and are represented by clinopyroxene (Cpx I), plagioclase (Pl I) and magnetite (Mgn) as magmatic assemblage and amphibole (Am I, and II) plagioclase (Pl II and III), pyrite and chalcopyrite as a metamorphic assemblage. Zoned amphiboles in magmatic and metabasic rocks have already been described

Table 2: Microprobe analyses of amphiboles from metagabbro, normalized to 22 oxygen atoms.

Sample No.	Oxides in Wt. %								
	SiO ₂	TiO ₂	Al ₂ O ₃	FeO	MnO	MgO	CaO	Na ₂ O	K ₂ O
M.M1c	50.3800	0.0000	6.1400	20.4200	0.0000	9.0600	12.1900	0.0000	0.0000
M.M1c	49.0300	0.0000	15.0200	37.2200	0.0000	2.6400	4.6200	0.0000	0.0000
M.M1c	50.9400	0.0000	6.2700	19.6100	0.0000	9.5900	12.2800	0.0000	0.0000
M.M1c	50.1600	0.0000	7.4800	19.5000	0.0000	9.0600	11.8100	0.0000	0.0000
M.M1c	50.2400	0.0000	6.9100	19.2300	0.0000	9.6400	11.6100	0.0000	0.0000
M.M1c	49.9700	0.0000	8.0900	18.1800	0.0000	8.7200	11.5000	0.0000	0.0000
M.M2r	51.9600		4.6500	20.0200	0.0000	10.4400	12.3500	0.0000	0.0000
M.M2c	45.7933	0.9983	9.0243	14.4428	0.1890	11.9850	12.0605	1.3644	0.6857
M.M2r	53.5021	0.3323	2.5169	11.2539	0.1650	16.4663	12.3959	0.4307	0.1344
M.M2r	50.5524	0.6132	4.1808	12.1819	0.2155	15.2048	12.3340	0.7907	0.1869
M.M2c	44.0771	2.7431	8.6205	14.2839	0.1836	11.6682	11.8378	1.9275	0.6356
M.M2c	52.9662	0.2900	2.0990	10.0399	0.2278	15.0793	16.3321	0.4935	0.0725
M.M2c	52.7787	0.3561	2.1237	10.0032	0.1581	15.1630	16.1013	0.4687	0.1213
M.M2c	50.4926	0.5050	3.9284	13.1784	0.1796	14.0572	12.0758	0.6124	0.2348
M.M5c	53.0740	0.3002	2.1538	12.6152	0.2513	15.5061	12.2135	0.4379	0.1130
M.M5r	42.7896	1.4008	9.8142	17.0308	0.2074	9.6688	11.5949	2.0283	0.7280
M.M5r	41.7707	1.2740	9.9835	18.0847	0.1885	9.2909	11.4597	1.6796	0.8036
M.M9r	42.3595	0.7407	11.4675	16.4067	0.2205	10.2386	11.7896	1.9206	0.7665
M.M9c	41.9517	0.8845	11.8887	16.7934	0.2466	9.4589	11.8174	1.8004	0.8506
M.M9c	26.2605	0.0000	19.9880	23.3485	0.2117	15.8300	0.0897	0.0000	0.0050
M.M9c	43.5688	0.5625	10.3600	16.2190	0.1861	9.9596	12.1368	1.3989	0.7413

and tested for evaluation of metamorphic conditions [31], [38] and [39] more rarely in metapelitic rocks [40] and [41]. Figure 8 shows a polished section of magnetite crystal in green schist. The magnetite crystal is surrounded by a pressure shadow containing amphibole and quartz. Pressure shadow is a region of low strain protected from deformation by a rigid euhedral or subhedral magnetite crystal [42]

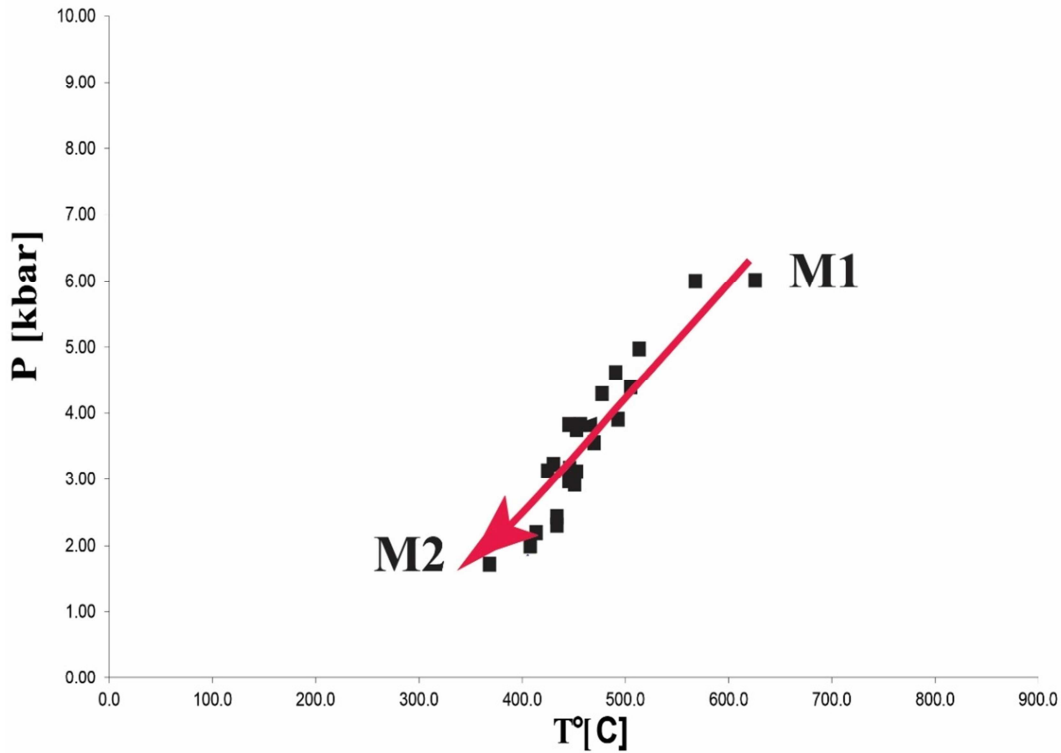


Figure 7: P-T condition of metagabbro estimated from amphibole equilibrium [24].

A number of parallel to subparallel NE-SW trending extension fissures are observed in polished section. Extension fissures are crack-like discontinuities formed perpendicular to the direction of the maximum incremental stretching as a result of brittle semi-brittle failure [42]. The direction of opening of their extension fissure is NW-SE (parallel or in the direction of the strike of the thrust sheets of the igneous complex). Accordingly, the direction of the maximum stretching strain ellipse in the study area is in the NW-SE direction. The suggestion support that the direction of the main driving force for the formation of the structure in the study area is in the NE-SW direction.

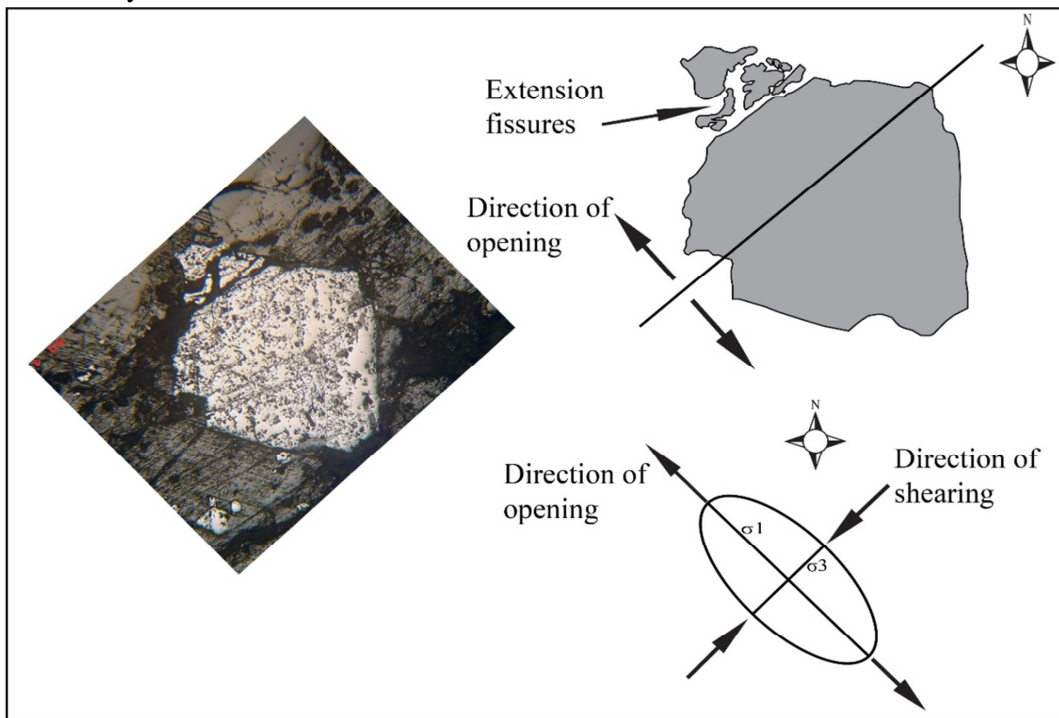


Figure 8: Microphotograph and sketch of magnetite mineral showing the strains and shearing direction.

Conclusions

Petrography and mineral chemistry show that the sheared gabbro underwent different stages of metamorphism. This is recorded by hornblende in the core rimmed with actinolite. This records a clockwise P-T-t path. The rocks initially passed through amphibolite facies ($500 < T < 560$ °C; $4.3 < P < 5.2$ kbar), followed by greenschist facies ($415 < T < 480$ °C; $1.9 < P < 2.3$ kbar).

Two types of primary mineralization occur in the Mirawa, sulfides which are represented by pyrite and chalcopyrite. The oxides are magnetite and ilmenite. They occur either as aggregates or disseminated and as vein fillings. Two stages of mineralization have been identified according to textural features (syntectonic and epigenetic). The alteration of these primary phase by supergene solutions forms secondary mineralization which are represented by covellite, hematite and goethite.

Detailed petrographic and microstructure observations reveal that formation of the Mirawa mineralization was related to magmatism and shearing as a result of Eocene crustal extension during the final stages of exhumation of a metamorphic rock complex.

References

- [1] Alavi, M. “*Tectonics of the Zagros orogenic belt of Iran: new data and interpretations*”, Tectonophysics Vol. 229, pp. 211–38. (1994).
- [2] Berberian, M., and King, G. C. P. “*Towards a paleogeography and tectonic evolution of Iran*”, Canadian Journal of Earth Sciences, Vol. 18, pp.210–65. (1981).
- [3] Mohajjel, M., and Fergusson, C.L. “*Dextral transpression in Late Cretaceous continental collision zone, western Iran*”, Journal of Structural geology Vol. 22, pp.1125–1139. (2000).
- [4] Mohajjel, M., Fergusson, C.L., and Sahandi, M.R. “*Cretaceous–Tertiary convergence and continental collision, Sanandaj–Sirjan Zone, western Iran*”, Journal of Asian Earth Science Vol. 21, pp. 397–412. (2003).
- [5] Agard, P., Omrani J, Jolivet L., Mouthereau, F. “*Convergence history across Zagros (Iran): Constraints from collisional and earlier deformation*”, International Journal of Earth Sciences Vol. 94, pp.401–419. (2005).
- [6] Stöcklin, J. “*Structural history and tectonics of Iran: a review*”, AAPG Bull, Vol.52, pp.1229 –1258. (1968).
- [7] Jassim, S. Z., and Goff, J. C. “*Geology of Iraq*” Prague and Moravian Museum Brno. pp. 341. (2006).
- [8] Fouad, S.F. “*Tectonic Map of Iraq, Scale 1:1,000,000, 3rded*”, GEOSURV: Baghdad, Iraq, (2010).
- [9] Williams, W. R. “*Mineral survey of mountains of north Iraq*”, GEOSURV, int. rep. No. 133. (1948).
- [10] Smirnov, V. A., and Nelidov, V. “*Report on 1:200000 prospecting correlation of Sulaimaniya, Chwarta, Penjwin area, Carried out in (1962)*”. GEOSURV, int. rep. No. 290, (1962).
- [11] Al-Hashimi, A. R., Al-Mehaidi, H. M. “*Cu-Ni-Cr dispersion in Mawat ophiolite complex, NE Iraq*”, Journal of Geology Society Iraq, special issue, pp. 37–44. (1975).
- [12] Mohammad, Y.O., Cornell, D.H., Qaradaghi, J.H., and Mohammad, F.O. “*Geochemistry and Ar–Ar muscovite ages of the Daraban Leucogranite, Mawat Ophiolite, Northeastern Iraq: implications for Arabia–Eurasia continental collision*” Journal of Asian Earth Science Vol. 86, pp. 151–165. (2014).
- [13] Vanecek, M. “*The principal metallogenic features of Iraq*” Acta Universitatis Caroliniae-Geologica Vol. 3, pp.237–252. (1972).
- [14] Ricou, L. E. Le “*Croissant Ophiolitique Peri-Arab: Une ceinture de nappes mises en place au crétacé supérieur*”, Rev. Geogr. Phys. Geol. Dyn., Vol (13) pp 327–349, (1971).
- [15] Al-Mehaidi, H. M. “*Tertiary nappes in Mawat range, NE Iraq*”, Journal of Geology Society Iraq, Vol. 7, pp. 31–44. (1975).

- [16] Buday, T. “*The regional geology of Iraq*”, in Stratigraphy and Paleogeography ed. by Kassab, I. M. and Jassim, S. Z., Dar Al-Kutub publishing house, Mosul, Iraq, Vol: I, pp. 445. (1980).
- [17] Buday, T., and Jassim, S. Z. “*The Regional Geology of Iraq*”, Tectonism, Magmatism, and Metamorphism. Geological Survey and Mineral Investigation of Baghdad, Vol 2, pp. 352. (1987).
- [18] Zakaria, M. B. M. “*Petrology and geochemistry of the southern part of Mawat ophiolite complex, northeastern Iraq*”, Unpubl. M. Sc. Thesis, University of Mosul. (1992).
- [19] Aswad, K. J., and Elias, E. M. “*Petrogenesis, geochemistry and metamorphism of spilitized subvolcanic rocks of the Mawat Ophiolite Complex, NE Iraq*”, Ofiolitti, Vol .13, pp. 95-109. (1988).
- [20] Ismail, S. A., Mirza, T. M., and Carr, P.F. “*Platinum-group elements geochemistry in podiform chromitites and associated peridotites of the Mawat ophiolite, northeastern Iraq*”, Journal of Asian Earth Sciences, Vol. 37, pp. 31–41, (2010).
- [21] Ali, S.A., Buckman, S., Aswad, K.J., Jones, B.G., Ismail, S.A. and Nutman, A.P. “*The tectonic evolution of a Neo-Tethyan (Eocene–Oligocene) island-arc (Walash and Naopurdan groups) in the Kurdistan region of the Northeast Iraqi Zagros Suture Zone*”, Island Arc Vol. 22, pp.104–125, (2013).
- [22] Azizi, H, Hadi, A., Asahara, Y., and Mohammed, Y.O. “*Geochemistry and geodynamics of the Mawat mafic complex in the Zagros Suture zone, northeast Iraq*”, Central European Journal of Geosciences Vol. 5, pp.523–537. (2013).
- [23] Hama-Aziz, N. R. “*Petrogenesis, evolution, and tectonics of the serpentinites of the Zagros suture zone, Kurdistan Region, NE Iraq*”, Unpublished PhD Thesis, Sulaimani University, Sulaimani, Kurdistan Region, Iraq, pp. 250. (2008).
- [24] Zenk, M., Schulz, B. “*Zoned Ca-amphiboles and related P-T evolution in metabasites from the classical Barrovian metamorphic zones in Scotland*”, Mineralogical Magazine Vol. 68, pp. 769-786. (2004).
- [25] Al-Hassan, M. E. “*Geochemistry and tectonic environment of dolomite rocks, Penjwin ophiolite complex, North east of Iraq*”, Iraqi Geological Journal. Vol. 29, No.1, pp. 50-63. (1996).
- [26] Radar, P. “*The Ore Minerals and their intergrowths*”. International series in earth sciences. Edited by Ingeson, D. E., Pergamon Press. Oxford. 2nd ed. Vol. 1 and 2, pp.1205. (1980).
- [27] Craig, J. R., and Vaughan, D. J. “*Ore Microscopy and Ore Petrography*”, John Wiley and Sons, New York, pp. 406. (1981).
- [28] Awadh, S. M. “*Mineralogy, geochemistry and origin of the Lead-Zinc-Barite deposits from selective areas from. North of Zakho, Northern Iraq*” Unpubl, Ph. D. Thesis, Baghdad University (2006).
- [29] Leake, B. E., Woolley, A. R., Arps, C. E. S., Birch, W. D., Gilbert, M. C., Grice, J. D., Hawthorne, F. C., Kato, F. C., Kisch, H. J., Krichovichev, V. G., Linthout, K., Laird, J., Mandarino, J. A., Maresch, W. V., Nickel, E. H., Rock, N. M. S., Schumacher, J.C., Smith, D. C., Stephenson, N. C. N., Ungaretti, L., Whittaker, E. J. W., Youzhi, G. “*Nomenclature of amphiboles: report of the subcommittee on amphiboles of the International Mineralogical Association, Commission on New Minerals and Mineral Names*”, American Mineralogist, Vol. 82, pp.1019-1037. (1997).
- [30] Rebay, G., and Messiga, B. “*Prograde metamorphic evolution and development of chloritoid-bearing eclogitic assemblages in subcontinental metagabbro (Sesia–Lanzo zone, Italy)*, Lithos, Vol.98, pp. 275-291. (2007).
- [31] Bégin, N. J., and Carmichael, D. M. “*Textural and compositional relationships of Ca-amphiboles in metabasites of the Cape Smith Belt, Northern Québec: Implications for a miscibility gap at medium pressure*”, Journal of Petrology, Vol. 33, pp. 1317–1343. (1992).
- [32] Triboulet, C. “*The (Na–Ca) amphibole–albite–chlorite–epidote–quartz geothermobarometer in the system S–A–F–M–C–N–H₂O. An empirical calibration*” Journal of Metamorphic Geology, Vol. 10, pp. 545–556. (1992).
- [33] Schulz, B., Triboulet, C., Audren, C., Pfeifer, H. R., and Gilg, A. “*Two-stage prograde and retrograde Variscan metamorphism of glaucophane-eclogites, blueschists and greenschists from Ile de Groix (Brittany, France)*”, International Journal of Earth Sciences, Vol. 90, pp. 871–889. (2001).

- [34] Horváth, P., and Árkai, P. “*Amphibole-bearing assemblages as indicators of microdomain-scale equilibrium conditions in metabasites: an example from Alpine ophiolites of the Meliata Unit, NE Hungary*”, *Mineralogy and Petrology*, Vol.84, pp.233–258. (2005).
- [35] Plyusnina, L. P.” *Geothermometry and geobarometry of plagioclase-hornblende bearing assemblages*”, *Contribution to Mineralogy and Petrology*, Vol.80, pp. 140–146, (1982).
- [36] Blundy, J. D., and Holland, T. J. B. “*Calcic amphibole equilibria and a new amphibole-plagioclase geothermometer*”, *Contribution to Mineralogy and Petrology*, Vol.104, pp. 208–224. (1990).
- [37] Holland, T. J. B., and Blundy, J. D. “*Non-ideal interactions in calcic amphiboles and their bearing on amphibole-plagioclase thermometry*”, *Contributions to Mineralogy and Petrology*, Vol.116, pp. 433–447. (1994).
- [38] Bachman, O., and Dungan, M. A. “*Temperature induced Al-zoning in hornblendes of the Fish Canyon magma, Colorado*”, *American Mineralogist*, Vol.87, pp. 1062–1076. (2002).
- [39] Schulz, B., Triboulet, C., and Audren, C. “*Microstructures and mineral chemistry in amphibolites from the western Tauern Window (Eastern Alps), and P-T-deformation paths of the Alpine greenschist-amphibolite facies metamorphism*”, *Mineralogical Magazine*, Vol. 59, pp. 641–659. (1995).
- [40] Vogl, J. J. “*Thermal-baric structure and P–T history of the Brooks Range metamorphic core, Alaska*”, *Journal of Metamorphic Geology*, Vol. 21, pp. 269–284. (2003).
- [41] Cruz, M. D. R. “*Zoned Ca-amphibole as a new marker of the Alpine metamorphic evolution of phyllites from the Jubrique unit, Alpujárride Complex, Betic Cordillera, Spain*”, *Mineralogical Magazine*, Vol. 74, pp.773–796. (2010).
- [42] Passchier, C., Trouw, R. A. J. “*Microtectonics.*”, 2nd^{ed}. Springer, Berlin Heidelberg, pp. 366, (2005).

